RSC Advances




ROYAL SOCIETY OF CHEMISTRY

www.rsc.org/advances

RSC Advances

RSCPublishing

COMMUNICATION

# Assembled nano-structures from micron-sized precursors

Cite this: DOI: 10.1039/xoxxoooooox

Bin Qian[‡a], Changhong Xiao[‡a], Ji Zou[a], Yuan Zhong[a], Zhijian Shen[a*]

Received ooth January 2014,
Accepted ooth January 2014

DOI: 10.1039/xoxxoooooox

www.rsc.org/

**Oriented assembly of small crystals to form larger structures are common in nature and a full understanding and control of such process would benefit the forthcoming nano-technologies. Such bottom-up assembly of nano-structures most often requires a precursor of nano-sized crystals. Here we demonstrate a novel laser sintering process that can rupture a submicron-sized zirconia precursor into nano-sized crystals, followed by a rapid oriented assembly of these small crystals. A detailed structure study has been carried out to understand the complex process and a model has been proposed. Such process sheds light on a new way of fabricating nano-materials using commercialized oxide materials.**

Self-assembly is the autonomous organization of components into patterns or structures without human intervention.[1-3] Such processes are abundant in nature and are of fundamental importance due to its involvement in many inorganic or bio-mineralization processes.[1,4-10] Self-assembly of nano-scaled components into tailored structures is believed to be a promising practical strategy for making nano-structures in solution or colloid systems. A similar process was observed in a more constrained environment, namely solid-state consolidation of oxides, where the self-assembly was described as ordered coalescence of nano-crystals.[11,12] Nano-sized crystallites ordered their crystallographic directions and built larger crystals in a way very different from the conventional grain growth mechanisms in solid state.[11-15] The self-assembly of ordered blocks (~$10^5$ atoms) instead of single atoms speeds the process tremendously and opens new ways also for making new composite nano-structures.[1] The common characteristic of all these mentioned self-assembling processes is using nano-sized precursors to form the larger size tailored structures. In this communication, we report the observation of a novel assembling process where the precursor is submicron-sized oxide grains. After rupture to nano-fragments by high-energy laser, these crystallites instantly gathered into assembled nano-structures. This laser induced rupture-assembling phenomenon is promising for preparation of materials with tailored deep structures.

A commercial 3 mol% yttria-doped zirconia powder (TZ-3Y-E, Tosoh Co., Ltd., Tokyo, Japan) was used as starting material. The received powder has an initial crystallite size of 27 nm (calculated by X-ray diffraction peak broadening) and an average particle size of ~45 nm (by microstructural observations). Dense beads with average size of 50-125 μm, consisting of grains of ~0.3 μm, were formed by freeze granulation followed by pressureless sintering. The beads were packed upon a flat support used for laser sintering. A Nd:YAG laser (wavelength 1064 nm) with a focused beam diameter of ~70 μm and a laser power of 20 W was used in this study. The laser beam shocks and fuses the zirconia beads following a pre-determined scan pattern calculated by Computer Aided Design (CAD) principle. A laser scanning speed of 50 mm/s and a hatched line separation of 0.05 mm was used. The entire laser sintering process is operated under argon atmosphere and the obtained sample shows black color. The achieved micro- and nano-scale microstructures were characterized by a Scanning Electron Microscope (SEM, JSM-7000F, JEOL, Tokyo, Japan) and a Transition Electron Microscope (TEM, FEG-2100F, JEOL, Tokyo, Japan). The Electron BackScatter Diffraction (EBSD) investigation was conducted using a digital HKL NordlysII F+ camera attached to a FEG-SEM Leo1530 upgraded to Zeiss Supra55. The cross section polishing was accomplished by using an argon ion beam polisher (SM-09010, JEOL, Tokyo, Japan) under the accelerating voltage of 6 KeV for 6 hours(without liquid nitrogen cooling). Specimens for TEM characterization were prepared mainly by cutting thin slices with well-polished surfaces by Argon ion beam slicer (EM-09100 IS, JEOL, Tokyo, Japan) and occasionally by fracture to study very thin fragment edges. X ray powder diffraction (PanalyticalX'Pert PRO) with reflection mode was used to obtain crystallographic phase information. Diffractograms were recorded from 40 to 120°(2θ) using monochromatic Cu Kα (λ=1.5405981 Å) radiation (40 mA, 45 kV).

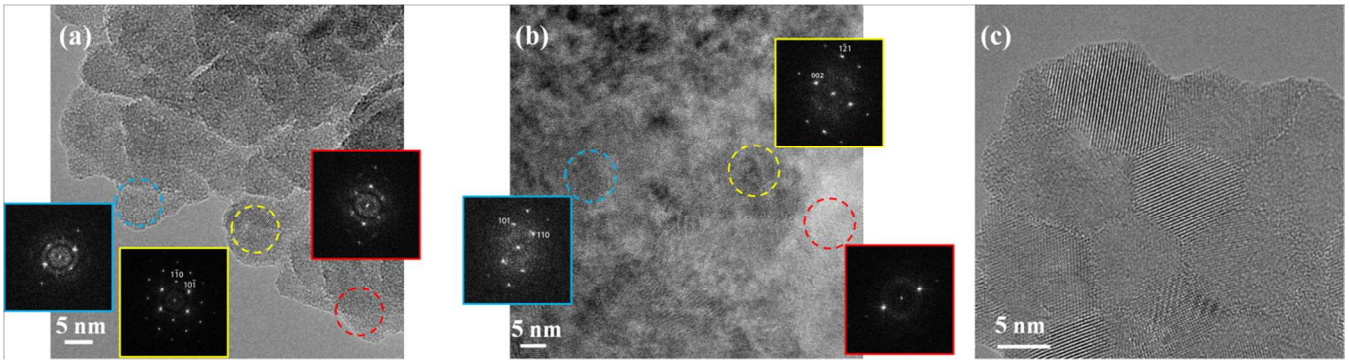


Fig. 3 HR-TEM images of the laser sintered $ZrO_2$ bulk. Image (a) and (b) are obtained inside one grain and on the grain boundary, respectively. Fourier Transform patterns at different sub-grain areas, marked by the three circles with corresponding colors, are inserted in both images. Image (c) is a HR-TEM image taken on a very thin fragment edge.

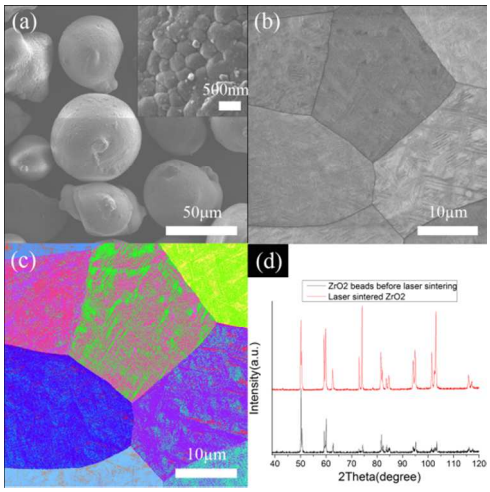


Fig. 1 The morphology and microstructure of the $ZrO_2$ powder beads before sintering are illustrated by SEM images in (a) with the inserted high magnification image revealing the constitutional grains of ~0.3 μm. A backscattered electron image revealing the microstructure of laser sintered $ZrO_2$ is shown in (b). An EBSD image taken on the same polished surface of a laser sintered $ZrO_2$ is found in (c), where the color diffidence denotes the crystal orientation difference. The XRD diagrams before and after laser sintering are presented in (d).

The morphology of the $ZrO_2$ beads before and the dense microstructure after laser sintering are shown in Fig. 1a and 1b, respectively. It can be seen that the initial small grains of ~0.3 μm underwent rapid growth to form large grains of ~20-30 μm in the laser sintered bulk. Because of the rapid laser scanning, the solidification and resulting grain structure is completed within one second. The curved grain shapes signposts that the grain boundary is under very high stress (or at high energy state). A variable grain contrast is clearly observed in backscattered electron image which might indicate an orientation difference at micro-scale. An electron backscatter diffraction (EBSD) image is taken to investigate crystallographic orientation changes between and inside the large grains (Fig. 1c). The obvious colour alteration shows a difference between the large grains. Inside these grains, however, the EBSD image indicates a further crystallographic orientation within the grains. A more detailed EBSD and amiss-orientation profile showed that a lot of 90 degree tetragonal twins existed. The presences of these twins are assumed as an effect of the rapid cubic-tetragonal $ZrO_2$ phase transition during the quick cooling process.[14-16] The sub-grain herringbone like contrasts found in back scattered electron images are consistent with the twin orientation differences seen by EBSD within the grains. The XRD diagrams of $ZrO_2$ beads before and the zirconia after the laser sintering process are shown in Fig. 1d. The XRD results indicate that the tetragonal phase is the dominating structure of $ZrO_2$ both before and after the laser sintering process. The stronger and sharper peaks from the sintered zirconia reveal that the ordered X-ray diffraction volumes are larger than the nano-sized precursor crystallites. Some orientation effects within the former are indicated by a slight variation of the relative peak intensity.

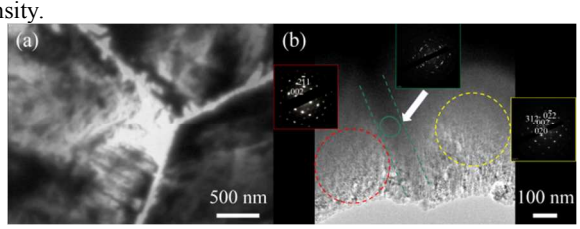


Fig. 2 The high magnification SEM image by secondary electrons (a) and the exposed TEM image at a grain boundary area of laser sintered $ZrO_2$ (b). The circles marked in the TEM image correspond to the selected areas for inserted electron diffraction patterns. The yellow and red circles are inside two separate grains while the green circle is within the grain boundary area marked by white arrows, *cf.* the text.

The high magnification SEM and TEM images of grain junctions are seen in Fig. 2a and b, respectively. By SEM the overall grain shape and a ~75 nm thick grain boundary zone between adjacent grains can be distinguished, see Fig. 2a. Owing to the small interaction volume, the second electron signal is very sensitive to the morphology of the top surface and a varying grain contrast is apparent. The Ar-ion milling, however, is gentle and produces a smooth surface in our experiments. The second electron signal is sensitive for their smaller energy and it has been reported that defects, such as oxygen vacancies, might influence the secondary electron emission yield which might influence the contrast.[17,18] In order to understand the origin of this contrast fluctuation, a detailed TEM study confirmed the presence of unusual wide less-ordered grain boundary zones in these dense materials, see the area marked by white arrows in Fig. 2b. The corresponding electron diffraction pattern gives mainly a polycrystalline signature. Inside the grains, the diffraction pattern

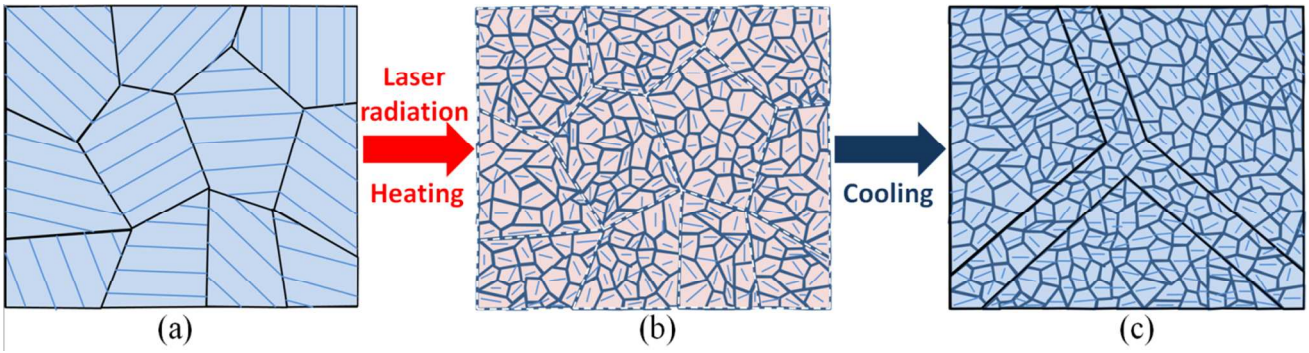


Fig. 4 The crystals before laser shock are illustrated with one crystallographic direction marked in (a). Laser energy gives extreme heating and ruptures in ~10 nm randomly oriented cubic crystallites within a solid grain in (b). After the instant rupture-assembling process new apparently 20-30 μm large "grains" with ~10 nm nano-crystals form separated by unusual wide (~50-100 nm) less-ordered zones in (c). The thin lines inside grains and crystallites represent the crystallographic orientation of these nano-crystals.

generally shows a single crystal feature. These crystallites are not perfect, however, as additional weak diffraction spots are found within the main diffraction pattern, see Fig. 2b. As we known, the tetragonal and cubic lattice parameters are very similar and only a small atom movement is needed to transform from one to the other. Thus, the shift from cubic to tetragonal structure can be achieved by any one of the three crystallographic axes becoming slightly longer. The crystalline phase formed immediately after solidification of the melt is cubic zirconia, which tends to transform to tetragonal zirconia when the temperature is cooled down to the tetragonal stability zone. Therefore, the transformation to a tetragonal phase is fully coherent with the cubic lattice on a nanometre scale and a lenticular morphology is usually seen. The addition of 3 mol% yttria would inhabit the further transformation to monoclinic phase. A careful check of the diffraction patterns shows that most, but not all, of the weak diffraction spots come from the three possible tetragonal variants. In order to understand the origin of the extra very weak diffraction spots, High Resolution TEM (HR-TEM) examination is performed. From HRTEM images it was found that the large $ZrO_2$ grains are built by assembling of nano-crystals with a size around 10 nm, as seen from an Ar-ion milled slice in Fig. 3a. Fast Fourier Transform (FFT) images established that these nano-crystals are aligned substantially in the same direction. At the wide grain boundary zone, the nano-crystal orientations form amore random pattern, as proved by the FFT image shown in Fig. 3b. This lattice disorder between nano-crystals is not consistent with the different tetragonal variants, originating from phase transformation, being 90 degree. In order to get rid of any possible artifact introduced by the Ar-ion milling process, images were also captured from very thin fragment edges, see Fig. 3c. Such an edge contains less overlapping crystallites and can show more details. The HR-TEM images verify the existence of an adjusted nano-crystalline structure within the bulk and the seen lattice fringes imply the nano-crystals orientations. The size of these nano-crystals is similar to that found in ion milled slices. The crystallite size of ~10 nm is small even compared with ordinary so called "ultra-fine grained materials",[19-22] which usually have grain sizes at least ten times larger. It should be pointed out that the observed zirconia represent a quenched non-equilibrium situation at nano level and the nanocrystals structural coherence by coalescence results in the appearance of well-ordered larger grains.

There are two magnitudes of microstructures found in the laser sintered zirconia. At micron scale, a modulated structure was formed within the large grains by the cubic to tetragonal phase transition.[15] This was manifested by the herringbone structure inside these grains observed by SEM in back scattered electron images and EBSD.

At a nano-meter scale, the grains were built by the assembling of nano-crystals, as revealed by HR-TEM. The thick grain boundary area separating grains is containing randomly orientated nano-crystals. The boundary is clearly seen in SEM by secondary electrons, by HR-TEM images and micro-EBSD; but less obvious using SEM at back scattering mode and macro-EBSD. The reasonable explanation is that the widespread well allied nano crystals weaken the contrasts seen by the two latter techniques. At the mean times, the grain boundary area holds more miss-orientated nano-crystals when compared with the ordering found inside each large grain.

The laser sintered samples are visually seen as black, which indicates the presence of oxygen vacancies or structural defects, such as slightly reduced zirconia with color centers.[17] The defects and color centers might be accumulated in the less ordered boundary zone, between the larger grains of ordered nano-crystals, as the latter have well-developed crystal boundaries. The formation of the inter-grain nano-structure seem not to fit with reported TEM observations of a transition between different tetragonal variants.[23] A long time aging process was needed for yttria-stabilized $ZrO_2$ and the reported modulated structures are not observed here. Still, the unusual wide grain boundary cannot be explained.[24,25] Here, we propose a new mechanism based on the unique heating history in the laser sintering process. The nano-structure is formed before the cubic to tetragonal phase transformation. A process called "ordered coalescence" is dominating the grain growth process. Zirconia is almost optical transparent in the Nd:YAG laser wavelength (1064 nm). Non-linear absorption is the main reason for the extreme heating within the $ZrO_2$ crystals during the laser scanning. This kind of absorption will be strongly inhomogeneous in the presence of any defects, such as color centers. At the meantime, the low oxygen content atmosphere and local high temperature assist a reduction reaction to release oxygen and form slightly reduced zirconia or more color centers. A strongly varied local heating will create huge short-distance temperature differences and subsequent thermal stresses that can rupture the materials structure. It might

also result in local partial melting at the defect position inside a grain that is different from other heating methods. The initial micro-sized $ZrO_2$ crystals will rupture vigorously into a huge amount of nano-crystallites (or partially melted crystallites) when interactions with the laser beam take place, see schematic illustration in Fig. 4b. Inside a solid state system this is an extremely unstable situation with considerable amounts of free crystal surface energy. An instant, strong strive will be to reduce the total surface by assembling nano-crystallites at crystallographic compatible arrangements. The induced high temperature provides enough kinetic energy for crystallite adjustments by movements and rotations. Owing to the following rapid cooling process, the nano-crystals bind by interfacial atomic bonds or adhesion, see in Fig. 4c. The defects would preferential exist in the nano-crystal boundary with broken chemical bonds or Zr at lower valence states. This ordered coalescence of nano-crystals results in grain growth and will freeze the nano-structure inside the new micron-grains. The phase transition from cubic to tetragonal zirconia is a secondary effect during the cooling. Within the grain boundary zone the crystalline orientation transit from one nano-crystal to another in a random way and will become thicker than a normally sintered glassy grain boundary. The nano-crystal boundary is a place suiting for "consuming" defects created by the laser process. This kind of ordered coalesce of nano-crystals is very promising for designing ultra-fine oxide materials.

In summary, a nano-structure is formed starting from submicron-size $ZrO_2$ grains and not from ultra-fine precursors. A novel mechanism which originals from the use of high-energy laser irradiation of zirconia, where the energy shock create a huge amount of ruptured~10nm crystallites in solid state. An instant ordered coalescence gave new apparently large grains of size ~20-30 μm in a solid material during rapid cooling, where each grain was composed of assembled ~10 nm nano-crystals.

## Acknowledgment

The work was supported by the Swedish Research Council. Support from the Knut and Alice Wallenberg foundation for the purchase of the laser sintering facility and electron microscopes used in this study are gratefully acknowledged. Authors would like to kindly thank Dr Erik Adolfsson for preparing the zirconia beads, thank Professors Thommy Ekström, Osamu Terasaki and Saeid Esmaeilzadeh for help and valuable comments.

## Notes and references

[a]Department of Materials and Environmental Chemistry, Arrhenius Laboratory, Stockholm University, 11418, Stockholm, Sweden

*Corresponding Author

Phone:+46-8-162388
Mobile:+46-70-8796488
Email address: shen@mmk.su.se

Author Contributions

‡These authors contributed equally.

1 G. M. Whitesides and B. Grzybowski, 2002, **295**, 2418.
2 J. C. Love, L. A. Etroff, J. K. Kriebel, R. G. Nuzzo and G. M. Whitesides,*Chem. Rev.,* 2005, **105**, 1103.
3 Z. Nie, A. Petukhova and E. Kumacheva, *Nat. Nanotechnol.,* 2010, **5**, 15.
4 J. M. García-Ruiz, E. Melero-García, S.T. Hyde, *Science,* 2009, **323**, 362.
5 S. Mann, *Nat. Mater.,* 2009, **8**, 781.
6 E. A. Kulp and J. A. Switzer, *J. Am. Chem. Soc.,* 2007, **129**, 15120.
7 C. Söllner, M. Burghammer, E. Busch-Nentwich, J. Berger, H. Schwarz, R. Christian and T. Nicolson, *Science,* 2003, **302**, 282.
8 H. Cölfen and S. Mann, *Angew. Chem. Int. Ed Engl.,* 2003, **42**, 2350.
9 L. Manna, D. J.Milliron, A. Meisel, E. C. Scher and A. P. Alivisatos, *Nat. Mater.,* 2003, **2**, 382.
10 Z. R. Tian, J. Liu, J. A. Voigt, B. Mckenzie and H. Xu, *Angew. Chem. Int. Ed.* 2003, **42,** 413.
11 S. Disch, E.Wetterskog, R. P. Hermann, G. Salazar-Alvarez, P. Busch, T. Brückel, L. Bergström and S. Kamali, *Nano Lett*., 2011, **11**, 1651.
12 D. Grüner and Z. J. Shen, *Cryst. Eng. Comm.,*2011, **13**, 5303.
13 J. F. Hu and Z. J. Shen, *Acta Mater.,* 2012, **60**, 6405.
14 C. Cayron, T. Douillard, A. Sibil, G. Fantozzi andS. Sao-Jao, *J. Am. Ceram. Soc.,* 2010, **93**, 2541.
15 R. H. J. Hannink, P. M. Kelly and B. C. Muddle, *J. Am. Ceram. Soc.,* 2000, **83**, 461.
16 A. Sibil, T. Douillard, C. Cayron,N. Godin, M. R'mili and G. Fantozzi, *J. Eur.Ceram. Soc.,*2011, **31**, 1525.
17 J. M. Costantini, A. Kahn-Harari, F. Beuneu and F. J. Couvreur, *Appl. Phys.,* 2006, **99**, 123501.
18 Y. Motoyama, *Plasma Sci. IEEE Trans.,* 2006, **336**.
19 L. Lu, M. L. Sui and K. Lu, *Science,* 2000, **287**, 1463.
20 M. H. Frey and D. A. Payne, *Phys. Rev. B,* 1996, **54**, 3158.
21 S. X. McFadden, R. S. Mishra, R. Z. Valiev, A. P. Zhilyaev and A. K. Mukherjee, *Nature,* 1999, **398**, 684.
22 C. Kleinlogel and L. J. Gauckler, *Adv. Mater.,* 2001,**13**, 1081.
23 T. Sakuma, Y. Yoshizawa and H. J. Suto, *J. Mater. Sci.,* 1986, **21**, 1436.
24 R. Chaim and D. J. Brandon, *J. Mater. Sci*., 1984, **19**, 2934.
25 M. Doi and T. Miyazaki, *Philos. Mag. Part B.,* 1993,**68**, 305.



 